HHS Public Access

Author manuscript

Proc SPIE Int Soc Opt Eng. Author manuscript; available in PMC 2018 January 22.

Published in final edited form as:

Proc SPIE Int Soc Opt Eng. 2015 February ; 9417: . doi:10.1117/12.2082124.

Nonlinear Functional Connectivity Network Recovery in the Human Brain with Mutual Connectivity Analysis (MCA): Convergent Cross-Mapping and Non-Metric Clustering

Axel Wismüller[1,2,3,4,*], **Anas Z. Abidin**[1,2], **Adora M. DSouza**[3], **Xixi Wang**[1,2], **Susan K. Hobbs**[1], **Lutz Leistritz**[5], and **Mahesh B. Nagarajan**[1,*]

[1]Department of Imaging Sciences, University of Rochester Medical Center, NY, USA

[2]Department of Biomedical Engineering, University of Rochester, NY, USA

[3]Department of Electrical Engineering, University of Rochester, NY, USA

[4]Department of Clinical Radiology, Ludwig Maximilian University, Germany

[5]Institute of Medical Statistics, Computer Sciences, and Documentation, Friedrich Schiller University Jena, Germany

Abstract

We explore a computational framework for functional connectivity analysis in resting-state functional MRI (fMRI) data acquired from the human brain for recovering the underlying network structure and understanding causality between network components. Termed mutual connectivity analysis (MCA), this framework involves two steps, the first of which is to evaluate the pair-wise cross-prediction performance between fMRI pixel time series within the brain. In a second step, the underlying network structure is subsequently recovered from the affinity matrix using non-metric network clustering approaches, such as the so-called Louvain method. Finally, we use convergent cross-mapping (CCM) to study causality between different network components. We demonstrate our MCA framework in the problem of recovering the motor cortex network associated with hand movement from resting state fMRI data. Results are compared with a ground truth of active motor cortex regions as identified by a task-based fMRI sequence involving a finger-tapping stimulation experiment. Our results regarding causation between regions of the motor cortex revealed a significant directional variability and were not readily interpretable in a consistent manner across subjects. However, our results on whole-slice fMRI analysis demonstrate that MCA-based model-free recovery of regions associated with the primary motor cortex and supplementary motor area are in close agreement with localization of similar regions achieved with a task-based fMRI acquisition. Thus, we conclude that our MCA methodology can extract and visualize valuable information concerning the underlying network structure between different regions of the brain in resting state fMRI.

[1] axel_wismueller@urmc.rochester.edu; phone 585-276-4775; University of Rochester, NY.

*Equal contributions.

Keywords

resting-state fMRI; functional connectivity; mutual connectivity analysis; convergent cross-mapping; non-metric clustering; Louvain method

1. INTRODUCTION

There has been significant growth in research aimed at exploring structural and functional connectivity in the human brain [1]. Of particular interest is the analysis of functional connectivity at fine-grained spatial and temporal resolution scales, based on the acquisition capabilities provided by advanced in vivo neuro-imaging techniques, such as state-of-the-art fMRI. Here, several contemporary analytic techniques such as seed-based functional connectivity analysis [2], independent component analysis [3], Granger causality [4], etc., imply inherent simplifications, such as assuming linearity or implicit time-series separability, which can obscure the characteristics of the complex system being investigated. Another drawback of such approaches is that they transform the original high-dimensional imaging data into simpler low-dimensional representations, which discards valuable information and thus limits the interpretability of brain connectivity analysis.

Our primary goal with this contribution is to introduce a computational framework for analyzing functional network connectivity of information transfer in the human brain, while simultaneously avoiding some of the information loss induced by the previously mentioned techniques. To this end, we present a mutual connectivity analysis (MCA) approach for non-linear functional connectivity analysis in large time-series ensembles obtained from resting state fMRI data. Our approach involves network identification through large scale non-linear mutual time-series cross-prediction [5] followed by functional network identification by partitioning the resulting affinity (or dissimilarity matrix) through non-metric clustering approaches, such as with the Louvain method [6]. Subsequently, causality analysis between identified network components is performed using convergent cross-mapping (CCM) [7].

We demonstrate the applicability of our MCA framework to identifying and visualizing the motor cortex through analysis of resting-state fMRI data. It has been previously shown that frequency fluctuations (< 0.1 Hz) from regions of the motor cortex associated with hand movement are strongly correlated both within and across hemispheres [2]. We explore non-linear connectivity and causality between time series ensembles from different regions of the motor cortex associated with hand movement, as discussed in the following sections. This work is embedded in our group's endeavor to expedite 'big data' analysis in biomedical imaging by means of advanced pattern recognition and machine learning methods for computational radiology, e.g. [8–38].

2. DATA

Functional MRI images were acquired from 4 healthy volunteers (1 female and 3 males, age range 25–28 years) with a 1.5T GE SIGNA™ whole-body MRI scanner (GE, Milwaukee, WI, USA). Two image sequences were acquired from each subject; the first was under resting state conditions while the second one involved a finger-tapping task stimulus to

localize the left motor cortex (LMC), right motor cortex (RMC), and supplementary motor area (SMA) regions for establishing ground truth (example shown in Figure 1). During the resting-state scan, the subject was instructed to stay still and keep eyes closed. The fMRI sequences were performed with the following parameters - echo time (TE) - 40 ms, echo-repetition time (TR) - 500 ms, and flip angle (FA) - 90°. 512 fMRI scans were acquired from two slice locations that corresponded to the motor cortex; each image had a slice thickness of 10 mm and an in-plane pixel resolution of 3.75 mm x 3.75 mm. The first 24 time points of fMRI data were discarded to avoid any impact on the data analysis by initial saturation effects.

3. METHODS

3.1 Pre-processing

Motion artifacts were compensated by automatic image alignment and signal drifts were corrected with linear de-trending. In addition, resting state fMRI time series were subject to low pass filtering with a cut-off frequency of 0.08 Hz for minimizing the influence of respiratory and cardio-vascular oscillations while preserving the frequency spectrum pertaining to functional connectivity [2]. Finally, the time-courses were further normalized to zero mean and unit standard deviation to focus on signal dynamics rather than amplitude [39].

3.2 MCA - Pair-wise Affinity Evaluation

Our first step is to build a pair-wise affinity/similarity matrix **A** for all time series of brain pixels on a single fMRI slice. Given n pixels, the pair-wise affinity between two pixel time series $\boldsymbol{X}$ and $\boldsymbol{Y}$ (where $\boldsymbol{X},\boldsymbol{Y} \in \{\boldsymbol{X}_k, k=1\ldots,n\}$) describes the degree of their dynamic coupling as a measure of their cross-prediction performance. For example, to compute matrix element $(\mathbf{A})_{\boldsymbol{X},\boldsymbol{Y}}$, we break down time series $\boldsymbol{X}$ of length l into a set of vectors $\mathbf{x}_i$, $i \in \{1,2,\ldots l-d+1\}$ of dimension d, which can be interpreted as a sliding window of length d moving along $\boldsymbol{X}$. The corresponding target vectors for $\mathbf{x}_i$ are $\mathbf{y}_i$ of dimension e. In this study, the parameters d and e were chosen $d=10$ and $e = 1$. Here, $\mathbf{x}_i$ is mapped to future $\mathbf{y}_i$, e.g. the vector $\mathbf{x}_i$ that comprises of the first 10 time points of $\boldsymbol{X}$ is mapped to $\mathbf{y}_i$ which corresponds to the 11th time point of $\boldsymbol{Y}$.

Using all (or a smaller sub-sampled set) of vectors $\mathbf{x}_i$, we can use a local simplex model, e.g. [7], to compute estimates $\hat{\mathbf{y}}_i$ of $\mathbf{y}_i$. Here, $d+1$ nearest neighbors $\mathbf{x}_j$ are identified for every $\mathbf{x}_i$. An estimate of its corresponding target vector $\hat{\mathbf{y}}_i$ is then computed as the weighted average of the target vectors for the $d+1$ neighbors. Thus,

$$\hat{y}_i = \sum_{j=1}^{d+1} w_j \, y_j,$$

where the weights w_j are determined as -

$$w_j = \frac{e^{-\|x_i - x_j\|^2 / \|x_i - x_1\|^2}}{\sum e^{-\|x_i - x_j\|^2 / \|x_i - x_1\|^2}}$$

Note that x_1 indicates the nearest neighbor for a specific x_i and $\|\cdot\|$ represents the Euclidean distance between vectors. The estimates $\hat{\mathbf{y}}_\mathbf{i}$ are subsequently concatenated to reconstruct $\hat{\boldsymbol{Y}}$. One may also make use of other local linear or average models described in the literature for this step. $(\mathbf{A})_{\boldsymbol{X},\boldsymbol{Y}}$ is now computed as the correlation coefficient between the prediction $\hat{\boldsymbol{Y}}$ and the actual time series $\boldsymbol{Y}$. Further details can be found in [40].

3.3 MCA - Non-Metric Clustering

From the affinity matrix **A**, we use the Louvain method [6] to recover the underlying network structure through non-metric clustering. The Louvain method aims to find high modularity clusters in networks, where modularity is defined as the ratio of the density of intra-community node linkage to the density of inter-community node linkage. Modularity Q is defined as

$$Q = \frac{1}{2m} \sum_{i,j} \left[A_{ij} - \frac{k_i k_j}{2m} \right] \delta(C_i, C_j)$$

where A_{ij} represents the affinity between nodes i and j,

$$k_i = \sum_j A_{ij}$$

is the sum of affinities of nodes attached to i, C_i is the community to which node i is assigned, $\delta(u,v) = 1$ when $u = v$, and 0 otherwise, and

$$m = \frac{1}{2} \sum_{ij} A_{ij}$$ [41]

Thus, a complex network is decomposed into clusters with strong intra-community links and weak inter-community links. The algorithm involves an iterative process during which different nodes of the network are merged into larger communities if the modularity is improved as a consequence. The process is discontinued when no further improvement in modularity can be achieved. Further details pertaining to this clustering approach can be found in [6].

In order to avoid the creation of large super-communities that encompassed smaller and more interesting clusters, we also pursue an approach frequently applied in spectral clustering to make the affinity matrix sparser [42]. Specifically, we only consider the k most similar nodes for any given node i. Additionally, only mutual k most-similar nodes are considered, i.e., bi-directional links in the k most-similar nodes. In this study, $k = 100$ is

chosen empirically from preliminary analysis; this corresponds to approximately 20% of the nodes in the network in most cases. Similarity between clustering results and the ground truth was evaluated using the Dice coefficient [43].

3.4 MCA - Causality Analysis

We further extend MCA to include convergent cross-mapping (CCM) for investigating causality between different regions of the primary motor cortex network. CCM explores the phenomenon of causation in non-linear systems, where the ability of time series $\boldsymbol{X}$ to better predict (or "cross-map") $\boldsymbol{Y}$ with increasing time-series length L is investigated. The length L can be modified by choosing appropriate collections of vectors $\mathbf{x}_i$ and their targets $\mathbf{y}_i$. Thus, according to [7], observing the degree to which $\boldsymbol{X}$ and $\boldsymbol{Y}$ are cross-mapped over increasing L enables one to establish grounds for causation.

In this study, we restrict the examination of causation to specific regions of the motor cortex, as identified using the ground truth. Thus, MCA with both GLM is used to build a smaller affinity matrix involving pixels from the LMC, RMC and SMA alone. From the entire collection of vectors x_i from time series X, a randomly chosen subset (of 10–80%) can have different variations. So we compute an affinity matrix for 20 different variations of subsets of x_i, and use their average for CCM analysis.

For interpretation of results achieved with CCM causality analysis, we present a pair-wise regional visualization of presumed causal influences between the LMC, RMC and SMA. Thus, when comparing any two regions in the motor cortex network, each pixel of a specific region is assigned an influence score based on its cross-prediction performance with all pixels in the other region.

All procedures were implemented using MATLAB 8.1 (MathWorks Inc., Natick, MA, 2013). The Louvain method implementation was taken from [44].

4. RESULTS

4.1 Network Recovery

Figure 2 shows the results of recovering communities associated with the motor cortex from a single resting state fMRI slice through non-metric clustering of the MCA affinity matrix using the Louvain method [6]. As seen here, MCA with non-metric clustering is able to recover the community structure of bilateral primary motor cortices and the supplementary motor areas. The overlap between the recovered regions of the primary motor cortex and the ground truth, as characterized by the Dice coefficient, was 0.51.

4.2 Causality Analysis

Figure 3 shows a visualization of the results of pair-wise causality analysis between the LMC, RMC and SMA for the same image slice as in Figure 1. A specific direction of causation is noted between the different regions, i.e., both LMC and RMC appear to influence the SMA. However, such findings are not consistent on images from other subjects.

5. NEW AND BREAKTHROUGH WORK

We present a computational framework for analysis of functional connectivity in the brain from resting state fMRI data for purposes of recovering the underlying network structure and establishing causality. While other methodologies for assessing functional connectivity through fMRI exist, such as seed-based approaches [2], ICA [3], etc., our framework avoids certain shortcomings, such as assumptions of linearity, time-series separability, etc. We instead propose to use non-linear mutual connectivity analysis (MCA) to evaluate the pair-wise cross-prediction quality between resting state fMRI time series acquired from the human brain. Our results, as seen in Figures 2–3, suggest that such pair-wise affinity matrices can reveal valuable information concerning the underlying network structure and causation between functionally connected brain regions. To the best of our knowledge, this is the first publication in the literature, which introduces convergent cross-mapping (CCM) into the domain of functional MRI analysis. Beyond its immediate applications in computational neuroscience, neurophysiology, and clinical neurology, we conjecture that our MCA approach to analyzing the dynamics of large non-linear systems will be useful in many other research domains throughout science and engineering, ranging from information retrieval to systems biology.

For future outlook, one can investigate other methods such a neural networks and information theory measures to setup the pair-wise affinity (or dissimilarity) matrix. One may also use other methods of non-metric clustering such as agglomerative clustering [45], pair-wise clustering through deterministic annealing [46], topographic mapping of proximity data (TMP) [47], spectral clustering methods based on eigenvalue decompositions of graph Laplacians [48] etc., in place of the Louvain method.

6. CONCLUSION

We present a mutual connectivity analysis (MCA) framework for analysis of functional connectivity and causality in the brain from resting state fMRI data, which combines local non-linear time series prediction, such as by using a local simplex model, with non-metric clustering, such as the Louvain method, for recovering the underlying functional brain network structure, and convergent cross-mapping (CCM) for exploring causation between different network components. By successfully recovering the network structure of the motor cortex, the results observed in our study demonstrate the applicability of our method to exploring functional connectivity in the human brain.

This work is not being and has not been submitted for publication or presentation elsewhere.

Acknowledgments

This research was funded by the National Institutes of Health (NIH) Award R01-DA-034977. The content is solely the responsibility of the authors and does not necessarily represent the official views of the National Institute of Health. This work was conducted as a Practice Quality Improvement (PQI) project related to American Board of Radiology (ABR) Maintenance of Certificate (MOC) for Prof. Dr. Axel Wismüller. The authors would like to thank Prof. Dr. Dorothee Auer at the Institute of Neuroscience, University of Nottingham, UK, for her assistance with the fMRI data acquisition process. The authors would also like Prof. Dr. Herbert Witte of Bernstein Group for Computational Neuroscience Jena, Institute of Medical Statistics, Computer Sciences, and Documentation, Jena

University Hospital, Friedrich Schiller University Jena, Germany, Dr. Oliver Lange and Prof. Dr. Maximilian F. Reiser of the Institute of Clinical Radiology, Ludwig Maximilian University, Munich, Germany for their support.

References

1. Margulies DS, Böttger J, Long X, Lv Y, Kelly C, Schäfer A, Goldhahn D, Abbushi A, Milham MP, Lohmann G, Villringer A. Resting developments: a review of fMRI post-processing methodologies for spontaneous brain activity. Magnetic Resonance Materials in Physics, Biology and Medicine. 2010; 23(5–6):289–307.
2. Biswal B, Yetkin FZ, Haughton VM, Hyde JS. Functional connectivity in the motor cortex of resting human brain using echo-planar MRI. Magnetic Resonance in Medicine. 1995; 34:537–541. [PubMed: 8524021]
3. Beckmann CF, DeLuca M, Devlin JT, Smith SM. Investigations into resting-state connectivity using independent component analysis. Philosophical Translations of the Royal Society B: Biological Sciences. 2005; 360:1001–1013.
4. Zhou Z, Ding M, Chen Y, Wright P, Lu Z, Liu Y. Detecting directional influence in fMRI connectivity analysis using PCA based Granger causality. Brain Research. 2009; 1289:22–29. [PubMed: 19595679]
5. Wismüller A, Lange O, Auer DP, Leinsinger G. Model-free functional MRI analysis for detecting low-frequency functional connectivity in the human brain. Proceedings of SPIE Medical Imaging. 2010; 7624:1M1–8.
6. Blondel VD, Guillame J-L, Lambiotte R, Lefebvre E. Fast unfolding of communities in large networks. Journal of Statistical Mechanics: Theory and Experiment. 2008:P10008.
7. Sugihara G, May R, Ye H, Hsieh CH, Deyle ER, Fogarty M, Munch S. Detecting causality in complex ecosystems. Science. 2012; 338:496–500. [PubMed: 22997134]
8. Bunte, K., Hammer, B., Wismüller, A., Biehl, M. Neurocomputing. Vol. 73. Elsevier; 2010. Adaptive local dissimilarity measures for discriminative dimension reduction of labeled data; p. 1074-1092.
9. Wismüller A, Vietze F, Dersch DR. Segmentation with neural networks. Handbook of Medical Imaging. 2000:107–126.
10. Leinsinger G, Schlossbauer T, Scherr M, Lange O, Reiser M, Wismüller A. Cluster analysis of signal-intensity time course in dynamic breast MRI: does unsupervised vector quantization help to evaluate small mammographic lesions? Eur Radiol. 2006; 16(5):1138–1146. [PubMed: 16418862]
11. Wismüller, A., Vietze, F., Behrends, J., Meyer-Baese, A., Reiser, M., Ritter, H. Neural Networks. Vol. 17. Pergamon; 2004. Fully automated biomedical image segmentation by self-organized model adaptation; p. 1327-1344.
12. Hoole, P., Wismüller, A., Leinsinger, G., Kroos, C., Geumann, A., Inoue, M. Analysis of tongue configuration in multi-speaker, multi-volume MRI data. Proc. 5th Semin. Speech Prod. Model. Data CREST Work. Model. Speech Prod. Mot. Plan. Articul. Model; 2000. p. 157-160.
13. Wismüller, A. Ph D thesis. Technical University of Munich, Department of Electrical and Computer Engineering; 2006. Exploratory Morphogenesis (XOM): a novel computational framework for self-organization.
14. Wismüller, A., Dersch, DR., Lipinski, B., Hahn, K., Auer, D. ICANN 98. Springer; London: 1998. A neural network approach to functional MRI pattern analysis—clustering of time-series by hierarchical vector quantization; p. 857-862.
15. Wismüller, A., Vietze, F., Dersch, DR., Behrends, J., Hahn, K., Ritter, H. Neurocomputing. Vol. 48. Elsevier; 2002. The deformable feature map-a novel neurocomputing algorithm for adaptive plasticity in pattern analysis; p. 107-139.
16. Behrends, J., Hoole, P., Leinsinger, GL., Tillmann, HG., Hahn, K., Reiser, M., Wismüller, A. Bildverarbeitung für die Medizin 2003. Springer; Berlin Heidelberg: 2003. A segmentation and analysis method for MRI data of the human vocal tract; p. 186-190.
17. Wismüller A, Dersch DR. Neural network computation in biomedical research: chances for conceptual cross-fertilization. Theory Biosci. 1997; 116(3):229–240.

18. Bunte K, Hammer B, Villmann T, Biehl M, Wismüller A. Exploratory Observation Machine (XOM) with Kullback-Leibler Divergence for Dimensionality Reduction and Visualization. ESANN. 2010; 10:87–92.
19. Wismüller, A., Vietze, F., Dersch, DR., Hahn, K., Ritter, H. ICANN 98. Springer; London: 1998. The deformable feature map—adaptive plasticity for function approximation; p. 123-128.
20. Wismüller, A. Advances in Self-Organizing Maps. Springer; Berlin, Heidelberg: 2009. The exploration machine - a novel method for data visualization; p. 344-352.
21. Meyer-Bäse, A., Jancke, K., Wismüller, A., Foo, S., Martinetz, T. Eng Appl Artif Intell. Vol. 18. Elsevier; 2005. Medical image compression using topology-preserving neural networks; p. 383-392.
22. Huber, MB., Nagarajan, M., Leinsinger, G., Ray, LA., Wismüller, A. SPIE Med Imaging. Vol. 7624. International Society for Optics and Photonics; 2010. Classification of interstitial lung disease patterns with topological texture features; p. 762410
23. Wismüller A. The exploration machine: a novel method for analyzing high-dimensional data in computer-aided diagnosis. SPIE Med Imaging. 2009:72600G–72600G.
24. Bunte, K., Hammer, B., Villmann, T., Biehl, M., Wismüller, A. Neurocomputing. Vol. 74. Elsevier; 2011. Neighbor embedding XOM for dimension reduction and visualization; p. 1340-1350.
25. Wismüller, A. Advances in Self-Organizing Maps. Springer; Berlin Heidelberg: 2009. A computational framework for nonlinear dimensionality reduction and clustering; p. 334-343.
26. Huber, MB., Nagarajan, MB., Leinsinger, G., Eibel, R., Ray, LA., Wismüller, A. Med Phys. Vol. 38. American Association of Physicists in Medicine; 2011. Performance of topological texture features to classify fibrotic interstitial lung disease patterns; p. 2035-2044.
27. Wismüller A, Verleysen M, Aupetit M, Lee JA. Recent Advances in Nonlinear Dimensionality Reduction, Manifold and Topological Learning. ESANN. 2010
28. Wismüller, A., Meyer-Baese, A., Lange, O., Reiser, MF., Leinsinger, G. Med Imaging, IEEE Trans. Vol. 25. IEEE; 2006. Cluster analysis of dynamic cerebral contrast-enhanced perfusion MRI time-series; p. 62-73.
29. Twellmann, T., Saalbach, A., Muller, C., Nattkemper, TW., Wismüller, A. Detection of suspicious lesions in dynamic contrast enhanced MRI data. Eng. Med. Biol. Soc. 2004. IEMBS'04. 26th Annu. Int. Conf. IEEE; 2004. p. 454-457.
30. Schlossbauer, T., Leinsinger, G., Wismüller, A., Lange, O., Scherr, M., Meyer-Baese, A., Reiser, M. Invest Radiol. Vol. 43. NIH Public Access; 2008. Classification of small contrast enhancing breast lesions in dynamic magnetic resonance imaging using a combination of morphological criteria and dynamic analysis based on unsupervised vector-quantization; p. 56
31. Otto TD, Meyer-Baese A, Hurdal M, Sumners D, Auer D, Wismüller A. Model-free functional MRI analysis using cluster-based methods. AeroSense. 2003; 2003:17–24.
32. Varini, C., Nattkemper, TW., Degenhard, A., Wismüller, A. Breast MRI data analysis by LLE. Neural Networks, 2004. Proceedings. 2004 IEEE Int. Jt. Conf; 2004. p. 2449-2454.
33. Huber, MB., Lancianese, SL., Nagarajan, MB., Ikpot, IZ., Lerner, AL., Wismüller, A. Biomed Eng IEEE Trans. Vol. 58. IEEE; 2011. Prediction of biomechanical properties of trabecular bone in MR images with geometric features and support vector regression; p. 1820-1826.
34. Meyer-Base, A., Pilyugin, SS., Wismüller, A. Stability analysis of a self-organizing neural network with feedforward and feedback dynamics. Neural Networks, 2004. Proceedings. 2004 IEEE Int. Jt. Conf; 2004. p. 1505-1509.
35. Schlossbauer, T., Kallergi, M., Reiser, MF., Wismüller, A., Meyer-Baese, A., Lange, O., Leinsinger, G. J Electron Imaging. Vol. 15. International Society for Optics and Photonics; 2006. Segmentation and classification of dynamic breast magnetic resonance image data; p. 13020
36. Nagarajan, MB., Huber, MB., Schlossbauer, T., Leinsinger, G., Krol, A., Wismüller, A. Mach Vis Appl. Vol. 24. Springer; Berlin Heidelberg: 2013. Classification of small lesions in dynamic breast MRI: eliminating the need for precise lesion segmentation through spatio-temporal analysis of contrast enhancement; p. 1371-1381.
37. Nagarajan, MB., Huber, MB., Schlossbauer, T., Leinsinger, G., Krol, A., Wismüller, A. J Med Biol Eng. Vol. 33. NIH Public Access; 2013. Classification of Small Lesions in Breast MRI: Evaluating The Role of Dynamically Extracted Texture Features Through Feature Selection.

38. Wismüller, A., Meyer-Bäse, A., Lange, O., Auer, D., Reiser, MF., Sumners, D. J Biomed Inform. Vol. 37. Academic Press; 2004. Model-free functional MRI analysis based on unsupervised clustering; p. 10-18.
39. Wismüller A, Lange O, Dersch DR, Leinsinger GL, Hahn K, Pütz B, Auer D. Cluster analysis of biomedical image time-series. International Journal of Computer Vision. 2002; 46:103–128.
40. Wismüller A, Wang X, DSouza AM, Nagarajan MB. A Framework for Exploring Non-Linear Functional Connectivity and Causality in the Human Brain: Mutual Connectivity Analysis (MCA) of Resting-State Functional MRI with Convergent Cross-Mapping and Non-Metric Clustering. 2014 arXiv:1407.3809 [cs.NE].
41. Newman MEJ. Analysis of weighted networks. Physical Review E. 2004; 70:056131.
42. von Luxburg, U. Technical Report TR-149. Max Planck Institute for Biological Cybernetics; 2006. A tutorial on spectral clustering.
43. Dice LR. Measures of the Amount of Ecologic Association Between Species. Ecology. 1945; 26(3):297–302.
44. Scherrer, A. [Last accessed July 3, 2014] Community Detection algorithm based on Louvain method. (Version 1.0) [software]. Available from http://perso.uclouvain.be/vincent.blondel/research/Community_BGLL_Matlab.zip
45. Duda, RO., Hart, PE., Storck, DG. Pattern Classification. 2. John Wiley & Sons; 2001.
46. Hofmann T, Buhmann J. Pairwise data clustering by deterministic annealing. IEEE Transactions on Pattern Analysis and Machine Intelligence. 1997; 19:1–14.
47. Graepel T, OberMayer K. A Stochastic Self-Organizing Map for Proximity Data. Neurocomputing. 1999; 11:139–155.
48. Shi J, Malik J. Normalized cuts and image segmentation. IEEE Transactions on Pattern Analysis and Machine Intelligence. 2000; 22:888–905.

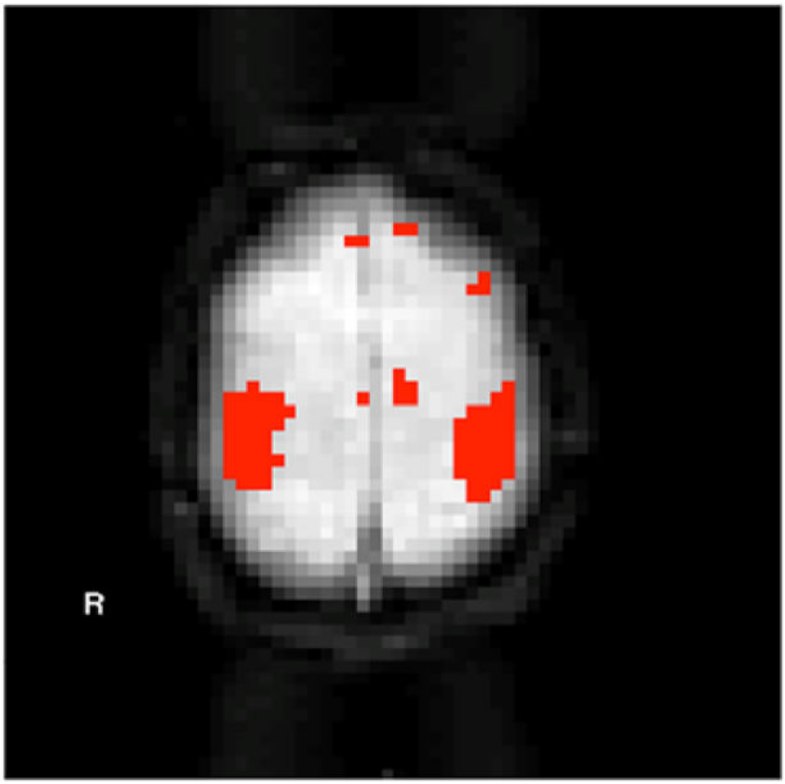

Figure 1.
The ground truth example for one subject. The identified primary motor cortex (left and right motor cortex) and pixels corresponding to the supplementary motor area (shown in red) are superimposed on the original slice.

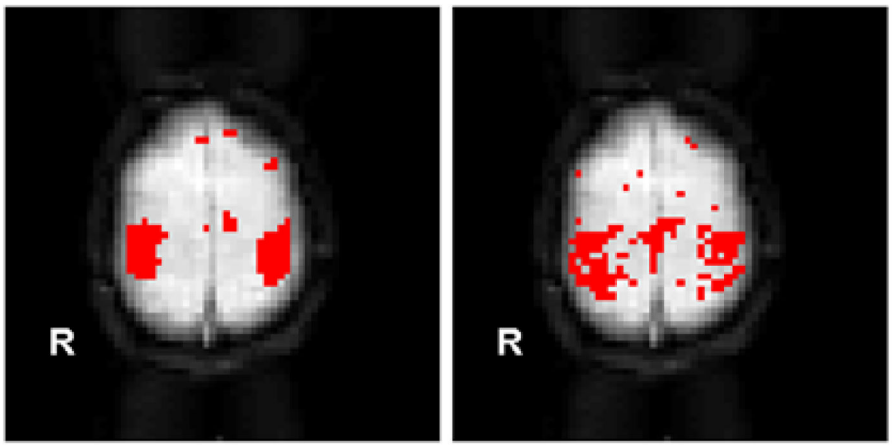

Figure 2.
(LEFT) Ground truth for primary motor cortex regions (LMC, RMC and SMA). (RIGHT) Motor cortex regions recovered from our MCA framework. Note the similarity of the identified brain networks revealing bilateral primary motor cortices and supplementary motor areas. Dice coefficient between the ground truth and our MCA network analysis results is 0.51.

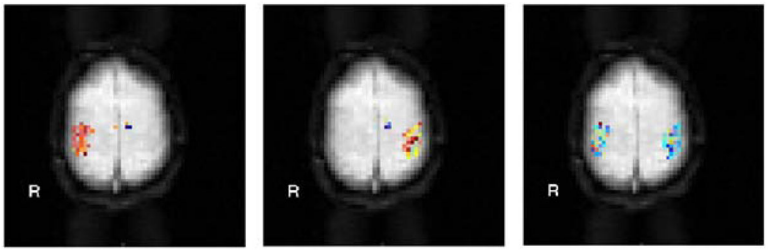

Figure 3.

Pair-wise regional causality analysis performed on a pixel-wise basis. From left to right, the pair-wise comparisons involve the RMC and SMA, LMC and SMA, and the LMC and RMC. The influence score of each pixel, as described in section 3.4 is color coded; red pixels are “influencers” while blue pixels are “influencees”.